04

Effect of plasma parameter profiles on a thermonuclear reaction operation

© Yu.V. Gott, E.I. Yurchenko

SRC „Kurchatov Institute“,
123182 Moscow, Russia
e-mail: Gott_YV@nrcki.ru

Received May 15, 2022
Revised August 1, 2022
Accepted August 27, 2022

The operation of a thermonuclear reactor on an alternative to D−T fuel (D−D, Cat−DD, D−^{3}He, p−^{11}B, p−^{6}Li) requires a higher temperature of the fuel mixture and an increased plasma energy confinement time. It is shown that at a fixed power of thermonuclear reaction, an increase in the peaking of plasma parameters leads to a decrease in power, which is necessary to its addition heating. Moreover, the peaking of the plasma parameters leads to decrease of its radiation losses. All this reduces the requirements for the operating conditions of thermonuclear reactor.

Keywords: thermonuclear reactor, alternative fuel, picking.

DOI: 10.21883/TP.2022.12.55190.135-22

Introduction

One of the alternatives to the currently existing energy is thermonuclear energy.

For a long time, it was believed that thermonuclear reactors operating on D−T mixtures are the most promising.

However, D−T-fuel has two significant drawbacks:

1) In the D−T reaction a large number of neutrons with energies of about 14 MeV are released, the flows of which lead to radioactive activation and destruction of surrounding structures [1].

2) There is no tritium in nature, and it must be produced in one way or another. Since tritium is radioactive, its use creates serious environmental and technological problems. Besides, the possibility of producing the required amount of tritium raises serious doubts.

These and other shortcomings call into question the implementation of an economically viable thermonuclear reactor [2–4].

Therefore, there is a need to create a reactor, which operation results in the minimum number of neutrons produced. For this purpose, thermonuclear reactions alternative to D−T reactions can be used: D−D, Cat−DD, D−^{3}He, p−^{11}B, p−^{6}Li and ^{3}He−^{3}He reaction, in which neutrons and tritium are not produced at all. The main thermonuclear reactions that may be of practical interest are listed below. The energy released during these reactions is also indicated there:

$$\mathrm{D}+\mathrm{D}\to\begin{cases}p+T+4.033\,\mathrm{MeV},\\ n+{}^3\mathrm{He}+3.269\,\mathrm{MeV},\end{cases}\tag{1}$$

$$\mathrm{D}+\mathrm{T}\to n+{}^4\mathrm{He}+17.589\,\mathrm{MeV},\tag{2}$$

$$\mathrm{D}+{}^3\mathrm{He}\to p+{}^4\mathrm{He}+18.353\,\mathrm{MeV},\tag{3}$$

$${}^3\mathrm{He}+{}^3\mathrm{He}=2p+{}^4\mathrm{He}+12.860\,\mathrm{MeV}.\tag{4}$$

It can be seen that the D−D reaction proceeds through two channels. The probability of these channels implementation is approximately the same.

The specific power of the energy released in the thermonuclear reaction has the form

$$W=\left(\frac{1}{2}\right)\frac{n_e^2}{4}E\langle\sigma v\rangle.\tag{5}$$

Here we assume that the density of the reacting elements is the same and the effective charge of the plasma is $Z_{\mathrm{eff}}=1$. In formula (5) n_e is electron density, $\langle\sigma v\rangle$ is reaction rate coefficient, E is energy released during thermonuclear reaction. The coefficient (1/2) in front of the formula appears when the same isotopes participate in the reaction. The values of $\langle\sigma v\rangle$ and W for the reactions under consideration are given in the Appendix.

For the convenience of comparison of the calculated data, we introduce the concept of profile peaking

$$\sigma_Z=\frac{Z(0)}{\langle Z\rangle},\tag{6}$$

where $Z(r)$ is any function that defines the plasma profile of temperature, concentration or pressure, $Z(0)$ is maximum value of the parameter, $\langle Z\rangle$ is value of the parameter averaged over the plasma volume.

The specific powers released in various reactions vs. the volume-averaged plasma temperature $\langle T\rangle$ are shown in Fig. 1. The calculations are performed for plasma, the density of which is equal to $n_e=1\cdot10^{14}\,\mathrm{cm}^{-3}$. It can be seen from the Figure that in all reactions the released power is much less than in the D−T reaction. Therefore, in order to obtain from the thermonuclear reactor a power comparable to that of the D−T reactor, it is necessary to heat the plasma

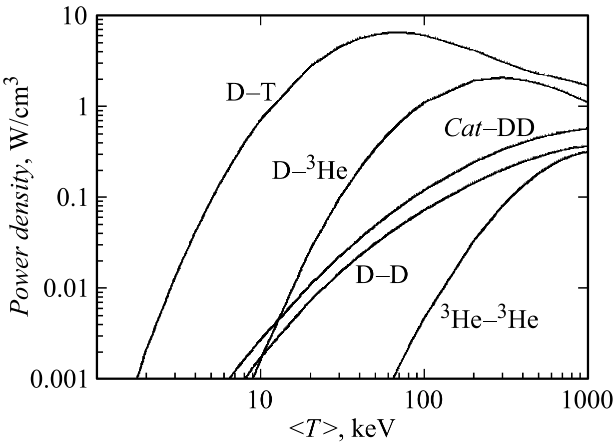

Figure 1. Specific power released during various types of thermonuclear reactions vs. average plasma temperature.

to higher temperatures. The work temperature increasing requires an increasing of the additional heating power.

Calculations show that the optimal plasma temperature at the center for the alternative fuel D–D, Cat–DD, D–^{3}He is 70–80 keV [5]. As the temperature decreases, the energy losses increase due to bremsstrahlung radiation, and upon the temperature rise energy losses increase due to cyclotron radiation.

The latter effect can be compensated by increasing β_T — ratio of gas-kinetic pressure of plasma to toroidal field pressure up to $\beta_T \sim 0.5$ for a spherical tokamak and even up to $\beta_T \sim 1$ for a tandem trap or trap with reversed magnetic field FRC [1,5–10].

For the reactions ^{3}He–^{3}He, p–^{11}B, p–^{6}Li, the optimal temperature is several hundred keV.

Usually, to determine the thermonuclear reactor characteristics the optimization is carried out with respect to various parameters of the plasma and the unit, such as plasma density and temperature, fuel composition, magnetic field strength, etc. But among these parameters there is practically no such parameter as the peaking of the plasma pressure.

It was usually assumed that in order to obtain the maximum production of thermonuclear energy, it is necessary to maintain the most uniform spatial distribution of plasma temperature and density in the reactor [11]. Actually, this is not the case. The use of steeper plasma profiles of temperature and density leads to time increasing of the energy confinement in the plasma [12–20], to the Lawson criterion decreasing [19], and decreasing of the ignition and combustion temperatures [20]. For example, in [18] it is experimentally shown that with density peaking increasing by 3 times in comparison with „flat“ distribution in L-mode the „triple“ distribution increased by 20 times, while the plasma confinement time increased by 3 times. Theoretical calculations carried out in [12] for the parameters of the T-10 unit showed that with the peaking of the plasma density increasing, the energy lifetime of the plasma increases approximately by 3.4 times. Besides, it was noted that in a strongly peaked plasma ignition can be achieved at a lower discharge current or at a lower power of additional heating [13]. As the peaking of the plasma pressure increases, the bootstrap current increases, the released thermonuclear plasma that was produced in the tokamak, increases, and the power required to maintain the current in the plasma decreases [14].

Estimates of the ignition factor $n\tau_E$ for the reactor operating on alternative fuel are given in [5]. Note that the energy lifetime of plasma increasing with the peaking of its parameters increasing can lead to weakening of the requirements for the power of its additional heating.

In this paper we consider the possibility of reducing the required energy content and, consequently, the power of additional heating of the plasma of the reactor operating on alternative fuel due to model profiling of its temperature and pressure.

For further estimates we assume that the working temperature for the reactions D–D, Cat–DD, D–^{3}He is 80 keV. Besides, the calculations were performed under the assumption that the number of particles in the entire plasma volume does not change, i. e., the average density $\langle n\rangle$ does not change.

A cylindrical plasma with a circular section of the plasma filament is considered.

1. Reactor using D–D-reaction

During D–D reactor operation the problems associated with tritium are reduced. Damage to structural materials in it is also much less than in the D–T reactor.

In Sec. 1, we will consider only the energy released in the reaction (1).

We will assume that the profiles of temperature and density of the D–D plasma are created by external sources (HF heating methods, injection of neutral beams, by pellet or gas puffing), and we will compare the generated energy for different profiles with the case of uniform distributions.

For simplicity of calculations, we set profiles of temperature and concentration that depend on one parameter only:

$$T = T_0(1-\rho^2)^{\mu_T} = \langle T\rangle(1+\mu_T)(1-\rho^2)^{\mu_T}, \qquad (7)$$

$$n = n_0(1-\rho^2)^{\mu_n} = \langle n\rangle(1+\mu_n)(1-\rho^2)^{\mu_n}. \qquad (8)$$

It follows from (7), (8) that the peaking of the profiles of temperature (σ_T) and concentration (σ_n) are equal to, respectively: $\sigma_T = 1+\mu_T$, $\sigma_n = 1+\mu_n$.

The magnitude of the pressure peak is described by a simple relationship

$$\sigma_p = 1+\mu_T+\mu_n. \qquad (9)$$

We will need this value in future. The peaking of the uniform distribution of parameters is equal to one. We will assume that the temperature and density of ions are equal to the temperature and density of electrons, i. e. $Z_{\text{eff}} = 1$. In

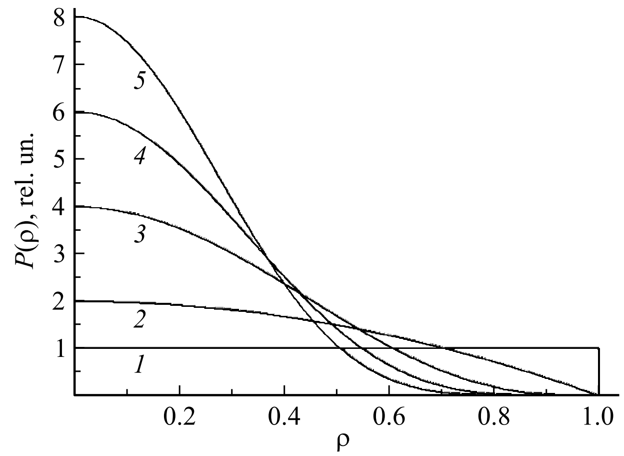

Figure 2. Radial dependences of plasma pressure on the peaking value σ_p. Curve *1* — uniform distribution of plasma pressure ($\sigma_p = 1$), curve *2* — $\sigma_p = 2$, curve *3* — $\sigma_p = 4$, curve *4* — $\sigma_p = 6$, curve *5* — $\sigma_p = 8$.

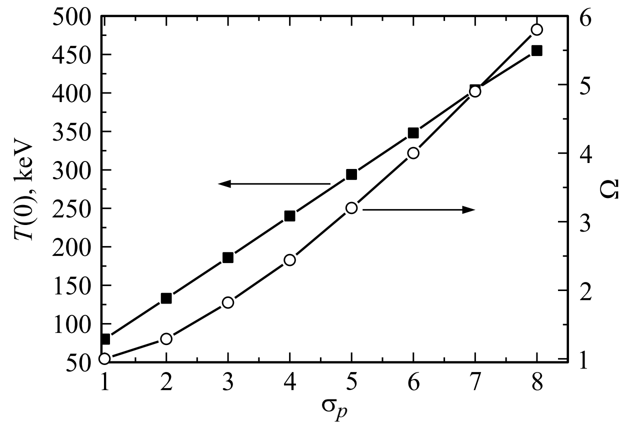

Figure 3. Temperature at the center of the plasma $T_p(0)$ and value Ω vs. σ_p while maintaining the total energy content in the D–D plasma.

this case, the energy content of the entire plasma Θ is equal to

$$\Theta = 3\langle n(\rho)T(\rho)\rangle V = 3\,\frac{n(0)T(0)}{\sigma_p}\,V$$

$$= 3\,\frac{\langle n(\rho)\rangle\langle T(\rho)\rangle\sigma_n\sigma_T}{\sigma_p}\,V, \tag{10}$$

where V is plasma volume. It can be seen from formulas (7), (8) that if the parameters distribution is known, then both the values of the parameters on the magnetic axis of the plasma and the values averaged over the volume can be used for analysis.

Further all values will be compared with the values for uniform distribution of plasma parameters with average temperature $\langle T\rangle_0 = 80\,\text{keV}$. The subscript 0 will be used for plasma with uniform distribution, and p — with peaked one. The thermonuclear energy released in the entire volume of the plasma, calculated by formula (5) for the temperature and concentration profiles given by (7)–(9), is equal to

$$W = A\int n^2E\langle\sigma v\rangle\,\rho d\rho = A\langle n\rangle^2\sigma_n^2E\int(1-\rho^2)^{2\mu_n}\langle\sigma v\rangle\rho d\rho. \tag{11}$$

Here A is normalization factor.

For uniform plasma distribution this energy is equal to

$$W_0 = A\int n^2E\langle\sigma v\rangle\rho d\rho = An^2(0)E\int\langle\sigma v\rangle\rho d\rho, \tag{12}$$

where the normalization factor A is chosen so that $W_0(80\,\text{keV}) = 1$. Note that for the uniform distribution $\sigma(0) = \langle\sigma\rangle_0$ and $T(0) = 80\,\text{keV} = \langle T\rangle_0$.

Thus, the normalized power of thermonuclear energy $\Omega = W/W_0$ is equal to

$$\Omega = \sigma_n^2\int(1-\rho^2)^{2\mu_n}\langle\sigma v\rangle\rho d\rho\Big/\int\langle\sigma v\rangle\rho d\rho. \tag{13}$$

Fig. 2 shows the radial dependences of the plasma pressure for various peaking values σ_p. Curve *1*in the Figure describes the uniform distribution of plasma pressure ($\sigma_p = 1$), curve *2* corresponds to $\sigma_p = 2$, curve *3* — $\sigma_p = 4$, curve *4* — $\sigma_p = 6$, curve *5* — $\sigma_p = 8$. It can be seen from the Figure that, as the peaking increases, the plasma pressure near the magnetic axis increases significantly.

Let us consider two cases:

a) When the peaking changes, the total energy content of the plasma is preserved, i.e., the values $\langle n\rangle$ and $\langle T\rangle$ are preserved.

Fig. 3 shows the normalized thermonuclear energy power Ω and the ion temperature at the center of the plasma column $T(0)$ vs. the plasma pressure peaking σ_p. It can be seen from the Figure that with the peaking increasing, both the normalized power and the ion temperature at the center of the plasma increase. For $\sigma_p = 9$ these values are equal to $\Omega = 5.8$ and $T(0) = 455\,\text{keV}$ respectively.

b) When the peaking changes, the normalized power $\Omega = 1$ is preserved.

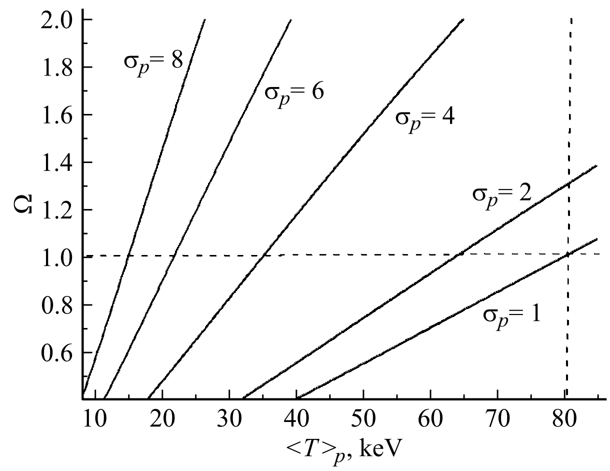

Figure 4. Relative specific reaction powers vs. average temperature of D–D-plasma for different values σ_p.

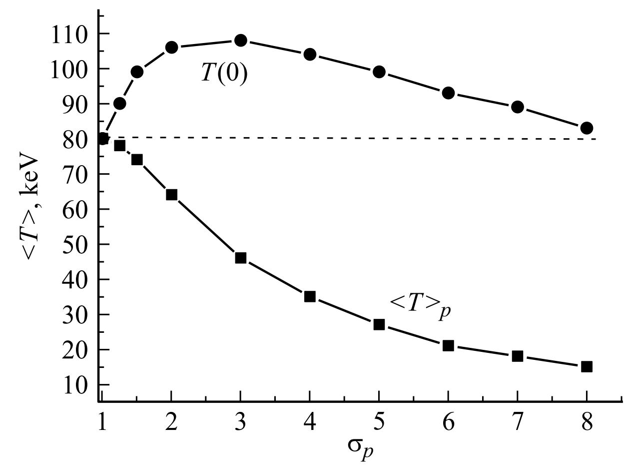

Figure 5. Temperature $\langle T\rangle_p$ and the temperature at the center of the plasma $T_p(0)$ vs. the pressure peaking of the D–D plasma σ_p.

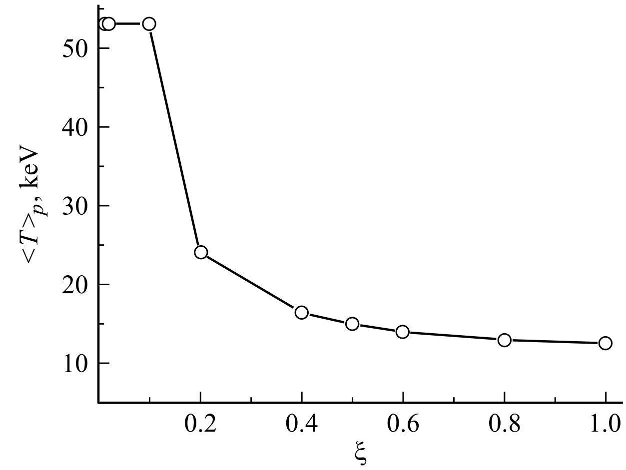

Figure 6. Temperature of D–D-plasma $\langle T\rangle_p$ vs. ξ.

Fig. 4 shows the results of calculations of Ω dependence on the average plasma temperature $\langle T\rangle_p$ for the same values of the pressure peaking shown in Fig. 2. The horizontal line marks the level of the released energy with uniform distribution over the section of the filament $\Omega_0(\langle T\rangle_0 = 80\,\text{keV}) = 1$.

The plasma temperature $\langle T\rangle_p$ at a given pressure peaking σ_p is determined by the point of intersection of the energy release curve Ω vs. $\langle T\rangle_p$ with the straight line defined by $\Omega_0(\langle T\rangle_0 = 80\,\text{keV}) = 1$.

The dependences of plasma temperature $\langle T\rangle_p$ and the temperature at the center of the plasma column $T(0)$ are shown in Fig. 5. It can be seen from the Figure that when peaking increases, the operating temperature decreases and reaches 15 keV at $\sigma_p = 8$. The temperature at the center of the plasma varies nonmonotonically, reaching $T_p(0) \approx 110\,\text{keV}$ at $\sigma_p = 3$ and decreasing to 83 keV at $\sigma_p = 9$. In this case, the energy content of the plasma decreases by 2.3 times. Thus, if for the plasma heating of the industrial reactor 3 GW, power of 300 MW [7] is required, then when the pressure peaking occurs, this power decreases to about 130 MW. For simplicity, we assume that the reactor parameters [7] were calculated for uniform distribution of the plasma density.

Fig. 6 shows the plasma temperature at $\sigma_p = 8$ vs. ξ, where $\xi = \mu_n/\mu_T$. It follows from the Figure that for a fixed peaking value ξ increasing to $\xi \sim 0.5$ leads to a strong decreasing of $\langle T\rangle_p$, and upon further $\xi\langle T\rangle_p$ increasing it changes slightly. Therefore, in this paper, the calculations were carried out at $\xi = 0.5$.

2. Reactor using *Cat*–DD-reaction

The reaction (1) is usually called the main D–D-reaction, and the reactions (2)–(4) are secondary. The energy released in the secondary reactions contributes to the total thermonuclear energy of the reactor. A set of reactions (1)–(4) is called a catalyzed *Cat*–DD-reaction.

In order to implement in practice the specific thermonuclear power of the *Cat*–DD reaction, which is increased in relation to the D–D-reaction, it is necessary either to eliminate the losses T and ^{3}He formed in reactions (1) or to inject additional amount of these isotopes into the plasma. To eliminate the neutrons generated in the reactor, tritium can be removed from it, and the power loss can be compensated by the additional injection of ^{3}He. Various options of *Cat*–DD-reactions are reviewed in detail in [5].

Let us consider the case when during D–D reaction T and ^{3}He remain in the plasma. Then such *Cat*–DD-reaction is described by formulas (1)–(4) and for $\sigma_p = 8$ the energy equal to the energy produced during uniform distribution with temperature $\langle T\rangle_0 = 80\,\text{keV}$ is generated at $\langle T\rangle_p = 11\,\text{keV}$. The temperature on the unit axis in this case is about 60 keV, and the required heating power decreases by about 2.9 times.

3. Reactor using D–^{3}He reaction

For D–^{3}He (3) reaction all other listed reactions are secondary, but their influence is usually neglected.

The neutron flux from a D–^{3}He reactor is approximately by two orders of magnitude less than from D–T reactor of the same power [1]. Note that such a reactor, producing 1 GW of electrical power per year, burns 100 kg ^{3}He and 67 kg of deuterium [21]. However, the complexity of its work lies in the fact that there is very little ^{3}He on Earth. A small amount of this isotope is found in natural gaseous helium. A certain amount of ^{3}He is dissolved in the ocean waters and contained in the earth's atmosphere. This isotope is also produced by the decay of tritium. Apparently, a lot of it is contained in the Earth's mantle, i. e., at distances from 30 to 2900 km from the Earth's surface, but this source is currently unavailable. It was expected [21] that in 2010 only 235 kg of ^{3}He will be produced on the Earth. If we assume that 5% of the fuel burns per year, then in this case, about 2 t of ^{3}He must pass through the reactor 1 GW per year. This shows that earth capabilities are insufficient to ensure the operation of even one power reactor. A large amount of ^{3}He is contained in the lunar regolith. Its production and transportation to the Earth for 2–3 millennia will provide its energy needs [21–24], and the cost of this process in energy equivalent can be comparable to the cost of oil [1,21].

The possibility of carrying out D–^{3}He reaction was already demonstrated in laboratory conditions [23].

However, the creation of such reactor encounters great difficulties, both technical and economic. Nevertheless, this problem may turn out to be a worthy task for the future development of thermonuclear studies, since the efficiency of thermonuclear energy production in the D–^{3}He reaction is noticeably higher than in the D–D reaction. For example, for $\langle T\rangle_p = 80\,\mathrm{keV}$ this value is approximately equal to 12.

Calculations show that for $\sigma_p = 8$ and $\langle T\rangle_p = 5.4\,\mathrm{keV}$ $T_0 \approx 31\,\mathrm{keV}$. The energy required to heat the plasma decreases by about 6.3 times.

The rest of the data qualitatively coincide with those obtained for the D–D reactor.

4. Reactor using ^{3}He–^{3}He-reaction

The thermonuclear reaction ^{3}He–^{3}He is remarkable in that neither neutrons nor tritium are produced in it, i. e., it is absolutely safe from the radiation point of view [1,25]

$$^3\mathrm{He} + {}^3\mathrm{He} = 2p + {}^4\mathrm{He} + 12.860\,\mathrm{MeV}, \tag{14}$$

The cross-section of this reaction is small, and therefore such reactors can only operate at very high plasma temperatures and high magnetic field strength.

It can be seen from Fig. 1 that power equal to that of D–D reactor operating at $\langle T\rangle = 80\,\mathrm{keV}$ can be obtained at $\langle T\rangle = 250\,\mathrm{keV}$, however, the peaking of the plasma parameters can significantly reduce the operating temperature. Thus, for $\sigma_p = 8$ it is $\langle T\rangle_p = 53\,\mathrm{keV}$ $(T(0) \approx 300\,\mathrm{keV})$, and for $\sigma_p = 16$ it reaches $\langle T\rangle_0 = 23\,\mathrm{keV}$ $(T(0) \approx 130\,\mathrm{keV})$.

5. Reactor using p–^{11}B-reaction

In addition to those discussed above, there are two more practically neutronless reactions, one of which is [26]

$$p + {}^{11}\mathrm{B} \rightarrow 3\,{}^4\mathrm{He} + 8.7\,\mathrm{MeV}. \tag{15}$$

This reaction (15) is not completely neutronless, since it is accompanied by the reaction

$$^4\mathrm{He} + {}^{11}\mathrm{B} \rightarrow {}^{14}\mathrm{N} + n + 0.2\,\mathrm{MeV}, \tag{16}$$

$$p + {}^{11}\mathrm{B} \rightarrow {}^{11}\mathrm{C} + n - 2.8\,\mathrm{MeV}. \tag{17}$$

The neutrons released in reactions (16) and (17) carry away approximately 0.1% of the thermonuclear power, which is almost by 800 times less than in D–T reactor.

Specific power released in reaction (15) vs. plasma temperature is shown in Fig. 7. The dependence for the

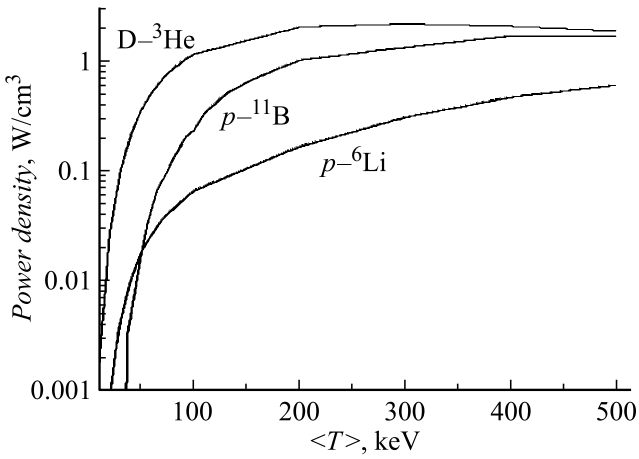

Figure 7. Specific power released during D–^{3}He- p–^{11}B- and p–^{6}Li-reactions vs. average plasma temperature.

D–^{3}He reaction is also shown there. It can be seen from the Figure that at temperatures exceeding $\langle T\rangle = 300{-}400\,\mathrm{keV}$, these powers differ little from each other. In [26] it is stated that the optimum temperature for p–^{11}B work is 300–400 keV. This temperature decreasing due to peaking of the plasma density can lead to two mutually opposite effects. One of them is increasing of the degree of ionization of boron and thus Z_{eff} increasing, hence losses increasing for bremsstrahlung radiation. Another effect is the plasma temperature decreasing due to increasing of its pressure peaking, which reduces the losses for bremsstrahlung radiation (see below). The final effect of the increased pressure peaking can only be determined as a result of additional analysis.

6. Reactor using p–^{6}Li reaction

Another neutronless reaction is the reaction [27]:

$$p + {}^6\mathrm{Li} \rightarrow {}^4\mathrm{He} + {}^3\mathrm{He} + 4\,\mathrm{MeV}. \tag{18}$$

Specific power released in reaction (18) vs. plasma temperature is shown in Fig. 7. It can be seen from the Figure that at the temperatures indicated on it the power is noticeably lower than the power of D–^{3}He- and p–^{11}B-reactors. Therefore, the plasma temperature in such reactor should be 0.8–1 MeV [27]. The authors of this paper state that the main obstacles to such reactor implementation can be bremsstrahlung and cyclotron radiation.

7. Radiative energy losses

Radiation losses are the losses of energy from the plasma due to cyclotron, bremsstrahlung and line radiation. In this paper, we will neglect the effect of line radiation, and consider cyclotron and bremsstrahlung losses based on the D–D reaction.

7.1. Cyclotron radiation

To estimate energy losses due to cyclotron radiation, we will use the expressions obtained in the papers [5,28–30].

On the one hand, the plasma concentration near the magnetic axis in case of peaking increasing leads to losses increasing due to cyclotron radiation. On the other hand, the plasma pressure increasing due to the diamagnetic effect reduces the magnetic field strength and thus leads to cyclotron losses decreasing. The approximate accounting of the diamagnetic effect is to replace the magnetic field strength B_0 by $B = B_0\sqrt{1-\langle\beta\rangle}$, where $\langle\beta\rangle$ is average value of the ratio of the gas-kinetic pressure of the plasma to the pressure of the magnetic field.

To estimate β vs. the radius, we use the relationship

$$\beta(\rho) \approx \beta_0(1-\rho^2)^{\sigma_p-1}, \tag{19}$$

where $\beta_0 = \langle\beta\rangle_0$, $\langle\beta\rangle_0$ is value under uniform pressure distribution.

The model value of the magnetic field vs. the radius, taking into account the diamagnetic effect, has the form

$$B(\rho) = B_0\sqrt{1-\beta(\rho)}. \tag{20}$$

Using the corresponding formulas from papers [5,28–30] to estimate the ratio of the radial dependence of the cyclotron radiation intensity to the average radiation intensity, we have

$$\Psi = \frac{W_{\mathrm{cycl}}(\rho)}{W_{\mathrm{cycl}\,0}} \approx \left[T(0)(1-\rho^2)^{\mu_T}/\langle T\rangle_0\right]^{2.5} \frac{\left(1-\beta(\rho)\right)^{1.25}}{\left(1-\langle\beta\rangle_0\right)^{1.25}}. \tag{21}$$

As can be seen, the changes in these losses are determined by the density and temperature peaking.

Fig. 8 shows the calculations of the radial dependence of the relative power of cyclotron radiation at $\sigma_p = 8$.

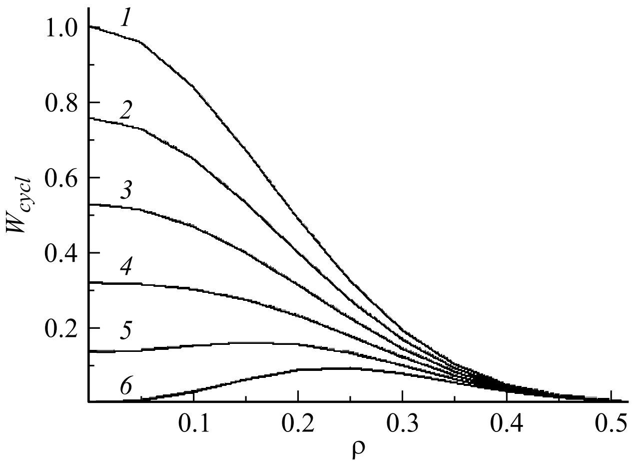

Figure 8. Radial dependence of the relative power of cyclotron radiation at $\sigma_p = 9$. Curve *1* — excluding the effect of diamagnetism ($\langle\beta\rangle = 0$), curve *2* — for $\langle\beta\rangle = 0.2$, curve *3* — for $\langle\beta\rangle = 0.4$, curve *4* — for $\langle\beta\rangle = 0.6$, curve *5* — for $\langle\beta\rangle = 0.8$, curve *6* — for $\langle\beta\rangle = 1$.

Curve *1* in the Figure describes the cyclotron radiation power for $\sigma_p = 8$ not considering the effect of diamagnetism ($\langle\beta\rangle = 0$). The remaining curves are plotted for different values of $\langle\beta\rangle$, i.e., taking into account the diamagnetic effect. Curve *2* — for $\langle\beta\rangle = 0.2$, curve *3* — for $\langle\beta\rangle = 0.4$, curve it4 — for $\langle\beta\rangle = 0.6$ and curve *5* — for $\langle\beta\rangle = 0.8$, curve *6* — for $\langle\beta\rangle = 1$. It can be seen from the Figure that the plasma peaking leads to a significant decreasing of the energy losses from the plasma due to cyclotron radiation. It can be seen from the data in Fig. 8 that at $\langle\beta\rangle = 1$, a region appears near the plasma axis from which the magnetic field is completely displaced, and, consequently, there is no cyclotron radiation from it.

Calculations by formula (21) show that in a unit operating on DD fuel, during pressure peaking $\sigma_p = 8$ the losses due to cyclotron radiation decrease by 16 times compared to losses from plasma with a uniform distribution.

In the reactor considered in [5], at $\beta_0 = 50\%$ and $T(0) = 80\,\mathrm{keV}$ the cyclotron losses are 30% of the generated thermonuclear power, i.e. $\sigma_p = 8$ peaking makes it possible to reduce these losses to 2%.

7.2. Bremsstrahlung radiation

The bremsstrahlung radiation power, taking into account the relativistic effect, can be represented as [5]:

$$W_{\mathrm{br}} = 5.35 \cdot 10^{-3}\, n_e^2(0) Z_{\mathrm{eff}}\sqrt{T(0)} X_{\mathrm{rel}} K_b\, \frac{\mathrm{W}}{\mathrm{cm}^3}. \tag{22}$$

Here, the electron density n_e is expressed in units of $10^{14}\,\mathrm{cm}^{-3}$, and the electron temperature T_e — in keV, X_{rel} — relativistic correction:

$$X_{\mathrm{rel}} = \left(1+\frac{2T_e(0)}{510}\right)\left[1+\left(\frac{2}{Z_{\mathrm{eff}}}\right)\left(1-\left(1+\frac{T_e(0)}{51}\right)^{-1}\right)\right], \tag{23}$$

where K_b — factor depending on the radial distribution of parameters:

$$K_b = \int n_e(r)T_e(r)X_{\mathrm{rel}}(\rho)dS \Big/ \left(n_e(0)T_e(0)X_{\mathrm{rel}}(0)\int dS\right). \tag{24}$$

Here, the integration is carried out over the plasma poloidal cross-section.

Since the power of thermonuclear energy (11) depends on density in the same way as the power of bremsstrahlung radiation (19), their ratio does not depend on density [6].

It follows from (22) that the ratio of energy losses due to bremsstrahlung radiation from plasma with a certain distribution of parameters to losses with uniform distribution is determined by the parameter K_b only. For $Z_{\mathrm{eff}} = 1.5$ and $\sigma_p = 8$ $K_b = 0.17$. Thus, it can be seen that in plasma with peaking $\sigma_p = 8$ the losses due to bremsstrahlung radiation decrease almost by 6 times compared to the losses from plasma with uniform distribution.

In DD-reactor at $T(0) = 80\,\mathrm{keV}$ and uniform distribution of plasma pressure the bremsstrahlung radiation power is by 3 times greater than the power of generated thermonuclear energy. Accounting for peaking reduces this value to 50%. For reactors with Cat–DD- and D–^{3}He-fuel, the ratio of energy losses due to bremsstrahlung radiation to thermonuclear energy becomes even smaller. Further losses decreasing due to bremsstrahlung radiation can be achieved by optimizing the main plasma parameters.

More exotic options like ^{3}He–^{3}He, p–^{6}Li, p–^{11}B require separate consideration.

It follows from the above analysis that in plasma with $\sigma_p = 8$ the losses due to cyclotron radiation can be neglected, and the bremsstrahlung radiation losses are also not a big problem.

Conclusion

1. The paper shows that the peaking of plasma parameters significantly affects the operation of the thermonuclear reactor.

2. The peaking increasing to generate the same thermonuclear energy leads to the plasma operating temperature decreasing in all considered types of reactors operating on alternative fuel.

3. The peaking increasing leads to the required plasma heating power decreasing.

4. The peaking increasing leads to the fact that the conditions of the thermonuclear reaction ignition are noticeably simplified.

5. Since when estimating the reactor parameters, they are usually optimized in terms of fuel composition, magnetic field strength, etc. [5], the results of this paper show that the plasma pressure peaking should be included in the composition of those values, according to which optimization is performed.

Acknowledgments

The authors consider it their pleasant duty to thank A.B. Kukushkin, P.V. Minashin, V.P. Pastukhov and A.Yu. Chirkov for helpful advice.

Conflict of interest

The authors declare that they have no conflict of interest.

Appendix

For the main five thermonuclear reactions (D–T, D–D, Cat–DD, D–^{3}He, ^{3}He–^{3}He) the reaction rate coefficient with an error, as a rule, not exceeding 10% for temperatures

Table 1. Values of coefficients a_i for formula (P2)

a_i	D–T	D–D	Cat–DD	D–^{3}He	^{3}He–^{3}He
a_0	−2.18297	−3.66139	−2.56458	−7.5241	−16.4943
a_1	6.20989	5.63857	3.10577	9.85941	17.94931
a_2	−2.36908	−2.46064	−0.48586	−3.8538	−8.6199
a_3	0.54067	0.63664	0	1.16414	2.69639
a_4	−0.22326	−0.07268	0	−0.32031	−0.46411
a_5	0.0448	0	0	0.03845	0.02804

Table 2. The value of the coefficient α for the formula (P3)

Reactions	D–T	D–D	Cat–DD	D–^{3}He	^{3}He–^{3}He
α	0.00704	0.00146	$\sim$ 0.00243	0.00736	0.00516

$0.086 < T < 862$ keV, can be represented as

$$\langle \sigma v \rangle \, 10^{18} = 10^u \ \mathrm{cm^3/s}, \tag{A1}$$

where

$$u = \sum_{i=1}^{3} a_i \theta^i, \tag{A2}$$

$\theta = \log_{10} T$, T temperature expressed in keV, $\log_{10}$ — decimal logarithm. The angle brackets denote averaging over the Maxwellian distribution. For D–T reaction formula P1 is valid up to energy of 500 keV.

The values of the coefficients a_i are presented in Table 1.

Approximation was performed according to the data of paper [31].

The specific power of the energy released in the listed reactions can be written in the following form:

$$W = \alpha n_e^2 \langle \sigma v \rangle \ \mathrm{W/cm^3}. \tag{A3}$$

Here, the electron density n_e is expressed in units $10^{14}\,\mathrm{cm^{-3}}$, and the rate coefficient — in units $10^{18}\,\mathrm{cm^3/s}$. The values of the α coefficients are given in Table 2.

References

[1] I.N. Golovin, B.B. Kadomtsev. Atomnaya energiya, **81** (5), 364 (1996). (in Russian)
[2] M. Ni, Y. Wang, B. Yuan, J. Jiang, Y. Wu. Fusion Engineering and Design, **88**, 2422 (2013). DOI: 10.1016/j.fusengdes.2013.05.043
[3] M. Kovari, M. Coleman, I. Cristescu, R. Smith. Nuclear Fusion, **58**, 026010 (2018). DOI: 10.1088/1741-4326/aa9d25
[4] Yu.V. Gott. Plasma Phys. Reports, **47**, 781 (2021). DOI: 10.1134/S1063780X21080043
[5] P.E. Stott. Plasma Phys. Control Fusion, **47**, 1305 (2005). DOI: 10.1088/0741-3335/47/8/011
[6] A.Yu. Chirkov. J. Fusion Energy, **32**, 208 (2013). DOI: 10.1007/s10894-012-9554-0

[7] D.C. Baxter, A.E. Dabiri, D. Dobrott, J.E. Glancy, H. Gurol, W.K. Hagan, J.B. McBride, S. Tamor, R.N. Cherdack. Nucl. Technol.—Fusion, **4**, 246 (1983). DOI: 10.13182/FST83-A22876

[8] K.Jr. Evans, C.C. Baker, J.N. Brooks, R.G. Clemmer, D.A. Ehst, P.A. Finn, H. Herman, J. Jung, R.F. Mattas, B. Misra, D.L. Smith, H.C. Stevens, L.R. Turner, R.B. Wehrle, K.M. Barry, A.E. Bolon, T. Robert, R.T. McGrath, L.M. Waganer. Nucl. Technol.—Fusion, **4**, 226 (1983). DOI: 10.13182/FST4-2P1-226

[9] A.Yu. Chirkov, V.I. Khvesyuk. V.I. Fusion Technol., **39**, 406 (20012). DOI: 10.13182/FST01-A11963491

[10] S.V. Ryzhkov. Fusion Sci. Technol., **55**, 157 (2009). DOI: 10.13182/FST09-A7004

[11] M.H. Redi, S.J. Zweben, G. Bateman. Fusion Technol., **13**, 57 (1988). DOI: 10.13182/FST88-A25085

[12] V.P. Pastukhov, D.V. Smirnov. JETP Lett., **114**, 208 (2021). DOI: 10.1134/S0021364021160086

[13] J.D. Tubbing, B. Balrt, D.V. Bartlett, C.D. Challis, S. Corti, R.D. Gill, C. Gormezano, C.W. Gowers, M. Von Hellermann, M. Hugon, J.J. Jacquinot, H. Jaeckel, P. Kupschus, K. Lawson, H. Morsi, J. O'Rourke, D. Pasini, F. Rimini, G. Sadler, G.L. Schmidt, D.F.H. Start, P.M. Stubberfield, A. Tanga, F. Tibone. Nucl. Fusion, **31** (5), 839 (1991). DOI: 10.1088/0029-5515/31/5/003

[14] D.R. Mikkelsen, K.M. McGuire, G.L. Schmidt, S.J. Zweben. Nucl. Fusion, **35**, 521 (1995). DOI: 10.1088/0029-5515/35/5/I03

[15] K. Ida, S.-I. Itoh, K. Itoh, S. Hidekuma, Y. Miura, H. Kawashima, M. Mori, T. Matsuda, N. Suzyki, H. Tamai, T. Yamauchi, JFT-2M Group. Phys. Rev. Lett., **68**, 182 (1992). DOI: 10.1103/PhysRevLett.68.182

[16] Yu.D. Pavlov, Yu.N. Dnestrovskij, A.A. Borshegovskij, V.V. Chistyakov, A.Yu. Dnestrovskij, M.M. Dremin, Yu.V. Gott, S.A. Grashin, E.P. Gorbunov, V.A. Zhuravlev, L.N. Khimchenko, A.V. Khramenkov, A.Ya. Kislov, S.V. Krylov, V.A. Krupin, S.E. Lysenko, V.V. Matveev, T.B. Mialton, V.V. Prut, I.N. Roy, D.A. Shelukhin, V.A. Vershkov, V.S. Zaveriaev. *28th EPS Conf. Controlled Fusion and Plasma Physics* (Portugal, Madeira, Funchal, 18–22 June, 2001, P4-020. ECA V.25A , 1409)

[17] F. Wising, D. Anderson, M. Lisak, M. Benda. Fusion Technol., **25**, 290 (1994). DOI:10.13182/FST94-A3

[18] K.M. McGuire, H. Adler, P. Alling, C. Ancher, H. Anderson, J.L. Anderson, J.W. Anderson, V. Arunasalam, G. Ascione, D. Ashcroft, C.W. Barnes, G. Barnes, S. Batha, G. Bateman, M. Beer, M.G. Bell, R. Bell, M. Bitter, W. Blanchard, N.L. Bretz, C. Brunkhorst, R. Budny, C.E. Bush, R. Camp, M. Caorlin, H. Carnevale, S. Cauffman, Z. Chang, C.S. Chang, C.Z. Cheng, J. Chrzanowski, J. Collins, G. Coward, M. Cropper, D.S. Darrow, R. Daugert, J. DeLooper, R. Dendy, W. Dorland, L. Dudek, H. Duong, R. Durst, P.C. Efthimion, D. Ernst, H. Evenson, N. Fisch, R. Fisher, R.J. Fonck, E. Fredd, E. Fredrickson, N. Fromm, G.Y. Fu, T. Fujita, H.P. Furth, V. Garzotto, C. Gentile, J. Gilbert, J. Gioia, N. Gorelenkov, B. Grek, L.R. Grisham, G. Hammett, G.R. Hanson, R.J. Hawryluk, W. Heidbrink, H.W. Herrmann, K.W. Hill, J. Hosea, H. Hsuan, M. Hughes, R. Hulse, A. Janos, D.L. Jassby, F.C. Jobes, D.W. Johnson, L.C. Johnson, M. Kalish, J. Kamperschroer, J. Kesner, H. Kugel, G. Labik, N.T. Lam, P.H. LaMarche, E. Lawson, B. LeBlanc, J. Levine, F.M. Levinton, D. Loesser, D. Long, M.J. Loughlin, J. Machuzak, R. Majeski, D.K. Mansfield, E.S. Marmar, R. Marsala, A. Martin, G. Martin, E. Mazzucato, M. Mauel, M.P. McCarthy, J. McChesney, B. McCormack, D.C. McCune, G. McKee, D.M. Meade, S.S. Medley, D.R. Mikkelsen, S.V. Mirnov, D. Mueller, M. Murakami, J.A. Murphy, A. Nagy, G.A. Navratil, R. Nazikian, R. Newman, M. Norris, T. O'Connor, M. Oldaker, J. Ongena, M. Osakabe, D.K. Owens, H. Park, W. Park, P. Parks, S.F. Paul, G. Pearson, E. Perry, R. Persing, M. Petrov, C.K. Phillips, M. Phillips, S. Pitcher, R. Pysher, A.L. Qualls, S. Raftopoulos, S. Ramakrishnan, A. Ramsey, D.A. Rasmussen, M.H. Redi, G. Renda, G. Rewoldt, D. Roberts, J. Rogers, R. Rossmassler, A.L. Roquemore, E. Ruskov, S.A. Sabbagh, M. Sasao, G. Schilling, J. Schivell, G.L. Schmidt, R. Scillia, S.D. Scott, I. Semenov, T. Senko, S. Sesnic, R. Sissingh, C.H. Skinner, J. Snipes, J. Stencel, J. Stevens, T. Stevenson, B.C. Stratton, J.D. Strachan, W. Stodiek, J. Swanson, E. Synakowski, H. Takahashi, W. Tang, G. Taylor, J. Terry, M.E. Thompson, W. Tighe, J.R. Timberlake, K. Tobita, H.H. Towner, M. Tuszewski, A. von Halle, C. Vannoy, M. Viola, S. von Goeler, D. Voorhees, R.T. Walters, R. Wester, R. White, R. Wieland, J.B. Wilgen, M. Williams, J.R. Wilson, J. Winston, K. Wright, K.L. Wong, P. Woskov, G.A. Wurden, M. Yamada, S. Yoshikawa, K.M. Young, M.C. Zarnstorff, V. Zavereev, S.J. Zweben. Phys. Plasmas, **2**, 2176 (1995). DOI: 10.1063/1.871303

[19] J. Kesner, R.W. Conn. Nucl. Fusion, **16**, 397 (1076). DOI: 10.1088/0029-5515/16/3/002

[20] B. Khosrowpour, N. Nassiri-Mofakhan. J. Fusion Energy, **35**, 513 (2016). DOI: 10.1007/s10894-016-0084-z

[21] T. Simko, M. Gray. World Future Review, **6**, 158 (2014). DOI: 10.1177/1946756714536142

[22] L.J. Wittenberg, E.N. Cameron, G.L. Kulcinski, S.H. Ott, J.F. Santarius, G.I. Sviatoslavsky, I.N. Sviatoslavsky, H.E. Thompson. Fusion Technol., **12**, 2230 (1992). DOI: 10.13182/FST92-A29718

[23] G.L. Kulcinski, H.Y. Schmitt. *Second Annual Lunar Development Conference „Return to the Moon II*" (Las Vegas, 20–21 July 2000)

[24] G.L. Kulcinski, R.P. Ashley, J.F. Santarius, G. Piefer, K. Murali. *ICEUM-4 Proc. Fowth Int Conf. on the Exploration and Utilisation of the Moon* (10–14 July 2000 ESA SP-462, Sept. 2000)

[25] J. Bahmani. Int. J. Hydrogen Energy, **45**, 16672 (2020). DOI: 10.1016/j.ijhydene.2020.04.107

[26] S.V. Putvinski, D.D. Ryutov, P.N. Yushmanov. Nucl. Fusion, **59**, 076018 (2019). DOI: 10.1088/1741-4326/ab1a60

[27] J. Bahmani, B. Eslami, F.M. Jafari. Int. J. Phys. Sci., **12**, 194 (2017). DOI: 10.5897/IJPS2017.4639

[28] A.B. Kukushkin, P.V. Minashin, V.S. Neverov. 22nd IAEA Fussion Energy Conf. Geneva. 2008. TH/P3-10.

[29] M. Mahdavi, T. Koohrokhi. Pramana, **74**, 377 (2010). DOI: 10.1007/s12043-010-0034-7

[30] F. Albajar, M. Bornatici, F. Engelmann. Nucl. Fusion, **49**, 115017 (2009). DOI: 10.1088/0029-5515/49/11/116017

[31] Y. Xu, K. Takahashi, S. Goriely, M. Arnould, M. Ohta, H. Utsunomiya. Nucl. Phys. A, **918**, 61 (2013). DOI: 10.1016/j.nuclphysa.2013.09.007.